International Journal for Housing Science and Its Applications
Publish August 6, 2025. Volume 46, Issue 3 Pages 4895-4906

https://doi.org/10.70517/ijhsa463419

Calculation and Optimization of Electric Vehicle Transportation Quantity of Roll-on Roll-off Vessel Combined with System Engineering Approach

Pan Shao[1,*], Daowang Ren[2] and Guoqi Ma[3]
[1] China Waterborne Transport Research Institute Beijing, Beijing, 100088, China
[2] Shandong Gangtong Engineering Consulting Co., Ltd, Yantai, Shandong, 264000, China
[3] Rizhao Transportation Bureau, Rizhao, Shandong, 276800, China
Corresponding authors: (e-mail: cxsp19860717@126.com).

Abstract Due to its characteristics of carrying passengers and vehicles, the passenger-roller ship needs to consider the safety performance and economic cost comprehensively. In this paper, ballast water is introduced as an indicator of economic cost when constructing the integer planning model of electric vehicle pre-allocation scheme for passenger-roller ships. At the same time, vehicle safety constraints and ship safety constraints are combined as safety performance indicators. The integrated cabin utilization rate and lateral overturning moment are modeled to balance the cabin loading capacity and stability. Combined with the pheromone attenuation mechanism of ant colony algorithm, the optimal computational solution of the loading scheme is carried out to maximize the benefits and minimize the risks of EV transportation on both passenger and ro-ro ships. The results show that the ant colony algorithm can achieve stable and fast convergence and the objective function value is smaller than the comparison algorithm when setting the information heuristic factor α, the expectation heuristic factor β, and the number of ants to 1.2, 2.0, and 65, respectively. In the 15 different scenarios of EV allocation schemes for passenger and roll-on/roll-off vessels based on the ant colony algorithm, the ship area utilization rate is more than 95%, and at the same time, the standard deviation is less than 0.005.

Index Terms ship area utilization, lateral overturning moment, ant colony algorithm, pheromone decay mechanism, loading optimization

I. Introduction

Roll-on/roll-off ship is a ship that realizes multiple functions such as loading cars and passengers at the same time as well as providing accommodation and entertainment services for passengers on board through functional partitioning of the deck [1], [2]. As a dual-purpose transportation ship, it integrates high speed, convenience, comfort and environmental protection, with high technological content, and is a high-end product in the world's shipping industry, with high loading and unloading efficiency, low requirements for wharves, low investment in ports, low loading and unloading costs, and "door-to-door" direct transportation and other advantages [3]-[6]. At the same time, there is a high cost of the ship, limited utilization rate of the cargo hold, safety and comfort performance requirements and other characteristics [7]. The above characteristics of passenger-roller ships make them show greater advantages in short- and medium-distance water transportation between seas, bays, straits, and coastal islands in economically developed regions, especially in the current society where the use of electric vehicles is soaring [8]-[11].

Electric vehicle is a new type of vehicle that uses all or part of the on-board battery as a power source and meets the requirements of road safety regulations, including pure electric vehicle (BEV), hybrid electric vehicle (HEV) and fuel cell electric vehicle (FCEv) [12]-[15]. In the electric vehicle transportation of passenger roll-on/roll-off ships, the reasonable loading and fastening of passenger roll-on/roll-off ship passenger vehicles is a major issue related to the navigation safety of passenger roll-on/roll-off ships [16]-[18]. A large number of facts show that due to the movement of the vehicle collision with each other caused by fire or the movement of the vehicle caused the ship to occur a large angle of the transverse tilt, resulting in the loss of ship stability and capsize, are related to the loading and fastening of the vehicle [19]-[21]. It can be seen that although the electric vehicle transportation of the passenger ship has the advantages of speed and quantity, but there are still hidden dangers from the electric vehicle, so the calculation and optimization of the number of electric vehicle transportation is of great significance for the safety of transportation [22]-[24].

This paper sets the minimization of ballast water usage and safe ship transportation as the objectives in the process of electric vehicle transportation by passenger-roller ship. Two vehicle safety constraint indicators, namely maximum transverse inclination angle of the ship and vehicle tethering angle, and two ship safety constraint indicators, namely transverse inclination moment of the ship and longitudinal inclination moment of the ship, are modeled and dynamically calculated. The ant algorithm based on path information density optimization is used to solve the optimization scheme of load distribution and realize the overall optimization of the transportation process. A large passenger-roller ship is selected for transportation optimization practice to test the advantages of the selected ant algorithm in practical application.

II. Technical analysis of the optimization of electric vehicle transportation on roll-on/roll-off vessels

This part comprehensively considers the needs of both EV transportation and cabin stabilization of passenger-roller ship, and analyzes the related algorithm implementation process.

II. A. Integral Planning Model for Rolling Stock Electric Vehicle Pre-allocation Schemes

II. A. 1) Optimization objectives

In planning the pre-allocation scheme for roll-on/roll-off vessels, minimizing the use of ballast water can reduce fuel consumption and shipping costs, and the use of ballast water is an important indicator for judging the economy of the pre-allocation scheme. When planning the pre-allocation program, when the weight of the vehicle on the deck can be distributed more evenly, the vehicle itself can be used as the effective weight of the ship to replace part of the weight of the ballast water, thus reducing the use of ballast water. Figure 1 represents the relationship between vehicle distribution and ballast water use. If the vehicles in Fig. (a) are concentrated on the right side, more ballast water needs to be injected into the ballast tanks on the left side of the ship to keep the ship in balance; compared with the distribution case in Fig. (a), the weight of the vehicles in Fig. (b) is distributed more uniformly, and then the ship uses very little ballast water. It can be seen that the distribution of vehicle weight on deck can represent the ballast water usage. In order to facilitate the calculation of the ship's ballast water use, this paper utilizes a ship balance indicator to measure the use of ballast water, and the closer the value of this indicator is to 0, the less ballast water is used on behalf of the ship. Calculation, to the vehicle deck layer center as the origin, the deck is divided into four quadrants of the same size, respectively, after loading the weight of the deck after the weight of each quadrant of the parked vehicle sum, through the calculation of the ship's balance indicator, so as to react to the ship's use of ballast water, which is referred to in this paper as the ballast water indicator.

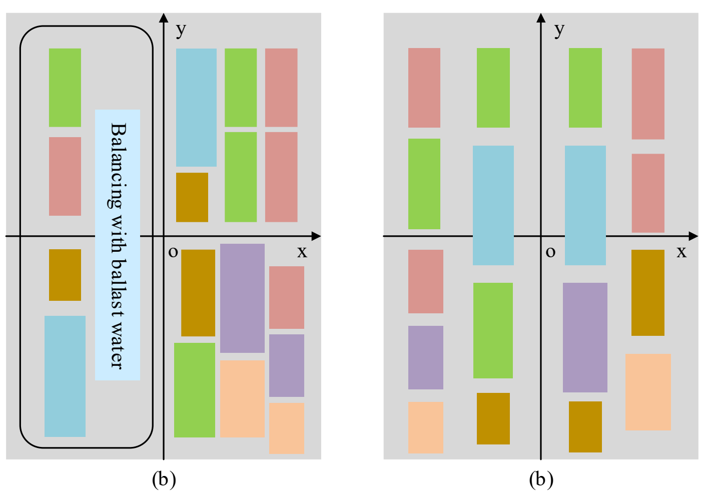

Figure 1: Vehicle position and ballast water usage

In order to improve the economy of the pre-allocation scheme, the use of ship ballast water is reduced through rational planning of the pre-allocation scheme, i.e., the ballast water index after the allocation of passenger and roll-on/roll-off ships is minimized, and the ballast water index is calculated by the formula:

$$\min \Delta = \min\left[\left(M_{q_1}+M_{q_3}-M_{q_2}-M_{q_4}\right)\cdot\left(M_{q_1}+M_{q_2}-M_{q_3}-M_{q_4}\right)\right] \tag{1}$$

$$M_{q_s} = \sum_{i \in q_s} m_i, s = 1,2,3,4 \quad (2)$$

The mathematical notations related to the integer planning model for the passenger-roller ship preloading scheme are described below:

(1) No.

i - serial number of the boarding vehicle, $i = 1,2,3.....n_t$;

j - body lashing point serial number, $j = 1,2,3,4$;

m_i - weight of vehicle i in t;

w_i - width of vehicle i, in m;

l_i - length of vehicle i, in m;

(2) Set

I_t - the set of serial numbers of vehicles that have boarded at moment t, numbered in order of boarding, $I_t \in K$, $I = \{i | i = 1,2,\cdots,k,|I|\}$;

(3) Parameters

N - total number of vehicles to be allocated;

L - length of the passenger-roller ship, unit: m;

B - width of the passenger-roller ship, unit: m;

W_d - deck width, in m;

L_d - deck length, in m;

g - acceleration of gravity in m/s^2;

T_x - maximum transverse moment of the ship, in $kN \cdot m$;

T_y - maximum longitudinal moment of the ship, in $kN \cdot m$;

(4) Auxiliary variables

Δ - ballast water indicator, the larger its value, the more ballast water is used;

q_s - quadrant s, $s = 1,2,3,4$;

M_{q_s} - the sum of vehicle gravity in quadrant s;

t - a moment in the loading phase of the vehicle, in s;

n_t - the total number of vehicles boarded at moment t, $n_t \le N$;

(x_i, y_i, z_i) - coordinates of vehicle i in cabin space;

KB_t - height of the ship's center of buoyancy at the moment t, in m;

BM_t - radius of the initial stability of the ship at the moment t, in units: m;

KG_t --Height of the center of gravity of the boarded vehicle at t moment, unit: m;

T_t - draft of the ship at t moment, unit: m;

Δ_t --displacement of the ship at t moment, unit: t;

θ_t - transverse inclination of the ship at the moment t, in °;

α_{ij} - tethering angle of vehicle i at body lashing point j, in °;

$\left(C_{ijx}, C_{ijy}, C_{ijz}\right)$ - the coordinates of vehicle i at body lashing point j in units of °;

$\left(D_{ijx}, D_{ijy}\right)$ - the coordinates of the deck ground order corresponding to the vehicle i body tie-down point j;

(5) Decision variables

K - the set of serial numbers of vehicles to be dispatched for embarkation, numbered sequentially in the order of embarkation, $K = \{k | k = 1,2,\cdots,N,|k|\}$.

II. A. 2) Constraints

When planning the pre-allocation scheme for passenger-roller ships, the safety of the vehicle during the loading process and the safety of the ship after loading need to be considered. The constraints involve the real-time state of the vehicle during the loading process and are characterized by dynamic calculation.

(1) Vehicle safety constraints

In the process of loading the ship, it is necessary to consider the safety of the vehicle traveling on the diving board; after completing the loading of the ship, it should measure the safety of the vehicle fastening on the deck.

The maximum transverse angle of the ship. When loading and unloading the passenger ship, the transverse angle is less than 4.5 ° to ensure that the normal work of the springboard, and the smaller the transverse angle is more conducive to vehicle safety. The transverse angle of the ship refers to the angle of transverse inclination of the ro-ro ship due to external force in the process of loading and unloading. As the ship loading is a dynamic process, the transverse inclination angle of the ship at t moment is closely related to the position of all vehicles on the ro-ro ship at that moment. The model takes the maximum value of the transverse inclination angle during the loading process in the calculation, and the formula is equation (3), and the constraint (4) indicates that the maximum transverse inclination angle of the ship should be within the specified range:

$$\max[\theta_t] = \arctan\left(\frac{GM_t}{B}\right) \tag{3}$$

$$-4.5^{\circ} \le \max[\theta] \le +4.5^{\circ} \tag{4}$$

Vehicle tie-down angle. Vehicle fastening angle (tied vehicle ropes and the deck of the acute angle) should be between 35 ° ~ 65 °, and the smaller the more conducive to preventing the vehicle translation, and vice versa will increase the possibility of ship capsizing and sinking. When the deck parking vehicle fastening angle are in the required range, take the fastening angle of the plural as the pre-loading program of the vehicle fastening angle value; when there is more than the required range of fastening angle, take the fastening angle of the maximum value of the vehicle fastening angle as the pre-loading program. Figure 2 shows the tether structure. The size of the tethering angle depends on the parking position of the vehicle and the ground order distribution of the deck, then the tethering angle α_{ij} at the i vehicle body lashing point j is calculated as equation (5), and the constraint (6) indicates that the tethering angle of the vehicle should be within a reasonable range:

$$\alpha_{ij} = \arctan\left[\frac{C_{ijz}}{\sqrt{\left(C_{ijx}-D_{ijx}\right)^2+\left(C_{ijy}-D_{ijy}\right)^2}}\right]\cdot\frac{180}{\pi} \tag{5}$$

$$35^{\circ} \le \alpha_{ij} \le 65^{\circ} \tag{6}$$

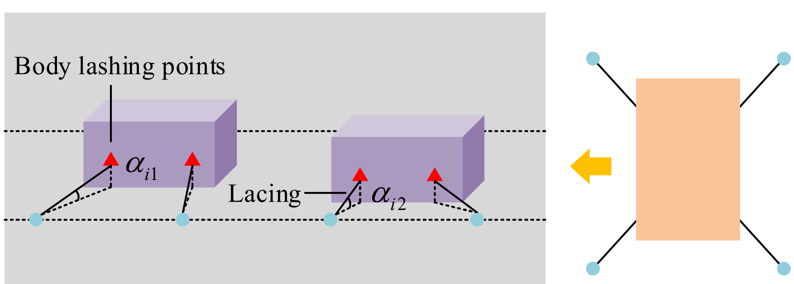

Figure 2: Vehicle fixed system schematic

(2) Ship safety constraints

This model measures the stability of the ship by the transverse and longitudinal moments of the ship after boarding is completed, and the smaller the absolute value is, the better the stability of the ship is. Since the ballast water tank capacity of a ro-ro ship is limited, it is necessary to ensure that the transverse and longitudinal moments of the ship are in the specified range to ensure that the use of ballast water is within the design range.

Ship transverse moment. Eq. (7) is the absolute value of transverse moment T_{tx} of the ship at the moment t, and the constraint (8) indicates that the value of transverse moment after completion of loading should be in the specified range:

$$T_{tx} = \left|\sum_{i=1}^{n_t}(m_i \cdot x_j \cdot g)\right| \tag{7}$$

$$\left|T_{tx}\right| \le T_x \tag{8}$$

Ship longitudinal moment. Equation (9) is the absolute value of the ship's longitudinal moment T_{ty} at moment t, and the constraint (10) indicates that the value of the longitudinal moment after completion of the loading of the ship should be within the specified range:

$$T_{ty} = \left| \sum_{i=1}^{n_t} (m_i \cdot y_i \cdot g) \right| \tag{9}$$

$$\left| T_{ty} \right| \le T_y \tag{10}$$

II. B. Calculation model of cabin utilization rate and cabin lateral overturning moment indicator

II. B. 1) Calculation of cabin utilization indicators

In this paper, the cabin utilization rate is used to represent the loading capacity of the ship's hold. Due to the need for fastening, a certain safety distance should be set aside when the vehicle is loaded, so the safety distance should be considered when the vehicle is loaded.

Suppose the width of the cabin is W and the length is L, given the R vehicles to be rowed, the length and width of any one of the vehicles are L_r and W_r respectively, the safety distance in the direction of the vehicle width is Δw, the safety distance in the direction of the vehicle length is Δl, the length of the vehicle after considering the safety distance is L_{r0}, and the width of the vehicle after considering the safety distance is W_{r0}.

The cabin utilization is calculated by equation (11):

$$U = \frac{\sum_{r=1}^{R} L_{r0} \times W_{r0}}{L \times W} \tag{11}$$

$$L_{r0} = L_r + 2\Delta l \tag{12}$$

$$W_{r0} = W_r + 2\Delta w \tag{13}$$

II. B. 2) Calculation of the index of lateral overturning moment of the cabin

Considering the navigation safety and avoiding the phenomenon of ship capsizing during navigation, the index of transverse capsizing moment must be considered when selecting the loading scheme, and after the loading is completed, the transverse capsizing moment of the ship refers to the algebraic sum of the capsizing moments generated by all the vehicles.

Assuming that the width of the cabin is W and the length is L, Figure 3 establishes the coordinate system. Coordinate origin O is located in the midpoint position of the line segment, there are R assigned vehicles in the cabin, using the center point coordinates to indicate each vehicle, the center point coordinates of the r th vehicle is (x_r, y_r), in order to facilitate the calculation of the transverse moment, the location of the vehicle is classified in terms of the relationship between x_r and 0, when $x_r < 0$, at this time, vehicle center point coordinates are located to the left of the origin; When $x_r \ge 0$, the coordinates of the vehicle center point are located on the right side of the origin or just at the origin, and the vehicle information is counted, assuming that the coordinates of the vehicle center point of the R_1 vehicle are located on the left side of the origin, the coordinates of the vehicle center point on the left side of the origin are $R_{i1} = (x_{i1}, y_{i1})$, and the vehicle mass is m_{i1}; There are a total of R_2 vehicles with vehicle center point coordinates to the right or just to the right of the origin, with vehicle center point coordinates $R_{j2} = (x_{j2}, y_{j2})$ and vehicle mass m_{j2}.

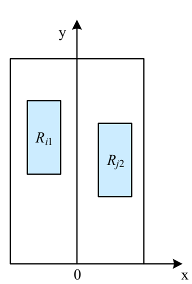

Figure 3: Coordinate System

The cabin lateral overturning moment F is shown in equation (14):

$$F = \sum_{i=1}^{R_1} x_{i1} m_{i1} g + \sum_{j=1}^{R_2} x_{j2} m_{j2} g \tag{14}$$

$$R = R_1 + R_2 \tag{15}$$

II. C. Modeling the Ant Colony Algorithm

II. C. 1) Path construction

Considering the electric vehicle transportation and loading of passenger and roll-on/roll-off vessels as a systematic project, an ant colony algorithm is used to optimally solve the engineering problem. In the computational model that simulates the behavior of ants searching for food in nature, each ant $k\left(k=1,2,\cdots,m\right)$ will decide its next moving direction based on the density of pheromones on the path when exploring. Compared to ants in nature, the artificial ants in the algorithm have memory capabilities, which allow them to use historical information to guide future decisions.

The memory of ant k is represented through the taboo table $tabu_k\left(k=1,2,\cdots,m\right)$, a mechanism that records the order of all nodes that ant k has passed through so far. During the search for the optimal solution, the ant will evaluate both the pheromone strength and the heuristic cues on the path to determine the likelihood of moving from position i to position j. The $p_{ij}^k(t)$ at time t reflects the transfer probability of ant k moving from location i to location j, i.e.

$$p_{ij}^k(t) = \begin{cases} \dfrac{\left[\tau_{ij}(t)\right]^{\alpha}\left[\eta_{ik}(t)\right]^{\beta}}{\sum_{s\in allowed_k}^{k}\left[\tau_{is}(t)\right]^{\alpha}\left[\eta_{is}(t)\right]^{\beta}}, j \in allowed_k \\ 0, Otherwise \end{cases} \tag{16}$$

where

η_{is} denotes the reciprocal of the distance between locations i and s.

$allowed_k = \{1,2,\cdots n\} - tabu_k$, when $allowed_k$ is null, it means that the ants have completed a tour. α reflects the importance of the pheromone, and the larger the value, the more ants previously choosing location j at location i, and the greater the probability that ant k tends to choose location j. β, on the other hand, reflects the importance of the distance between location i and location j, and the larger the value, the more ants tend to choose destinations that are closer to them.

II. C. 2) Pheromone updates

Figure 4 shows the general flow of the ant colony algorithm. After all the ants have completed the location visiting task, the algorithm updates the pheromone concentration of all the paths passed by the ants according to Eq. (17) and Eq. (18) at the moment $\left(t+n\right)$. In order to simulate the volatilization characteristics of ant pheromone in nature, the algorithm designs a pheromone decay mechanism so that it gradually decreases over time.

$$\tau_{ij}(t+n) = (1-\rho)\tau_{ij}(t) + \Delta\tau_{ij}(t) \tag{17}$$

$$\Delta\tau_{ij}(t) = \sum_{k=1}^{m} \Delta\tau_{ij}^k(t) \tag{18}$$

where $\rho\left(0<\rho<1\right)$ is the pheromone evaporation coefficient, and $\Delta\tau_{ij}^k(t)$ is the concentration of pheromone that ant k has left behind during this iteration.

For the value of $\Delta\tau_{ij}^k(t)$, Dorigo designed three different models, Ant-Cycle Model, Ant-Quantity Model and Ant-Density Model, which correspond to three forms of ant system algorithms.

1) Ant-Cycle Model

$$\Delta\tau_{ij}^{k}(t)=\begin{cases}\dfrac{Q}{L}, & \text{If the kth ant passes through } (i,j) \text{ in this cycle} \\ 0, & \text{Other}\end{cases} \quad (19)$$

where Q denotes the total amount of pheromone released by the ants during this search, and L is the total length of the path passed by the k th ant during this search.

2) Ant-Quantity Model

$$\Delta\tau_{ij}^{k}(t)=\begin{cases}\dfrac{Q}{d_{ij}}, & \text{If the kth ant passes through } (i,j) \text{ in this cycle} \\ 0, & \text{Other}\end{cases} \quad (20)$$

where d_{ij} denotes the distance between location i and location j.

3) Ant-Density Model

$$\Delta\tau_{ij}^{k}(t)=\begin{cases}Q, & \text{If the kth ant passes through } (i,j) \text{ in this cycle} \\ 0, & \text{Other}\end{cases} \quad (21)$$

The comparison reveals that the three models are different in that the Ant-Cycle Model utilizes the length of the path that the ants have traveled during this traversal to achieve pheromone updating; the Ant-Quantity Model utilizes the dynamic distances between the locations passed through to dynamically update the pheromone concentration; and the Ant-Density Model does not take into account the inter-location The Ant-Density Model does not consider the heuristic distance between locations, but rather fixes the pheromone increase on the path to a preset constant value. Among them, Ant-Cycle Model shows excellent efficiency and accuracy in solving the traveler problem.

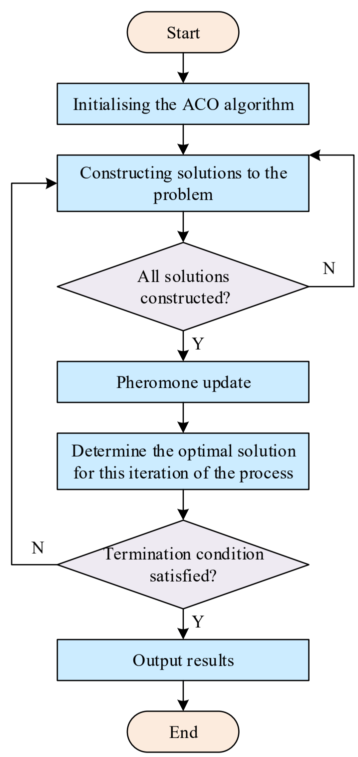

Figure 4: Ant colony algorithm flowchart

III. Optimization Practice of Electric Vehicle Transportation on Roll-on Roll-off Vessels

In this part, the electric vehicle transportation scheme of a large passenger ship is selected as the research object. After setting the optimal parameters of the used ant colony algorithm, it is applied to the optimization solution of the transportation allocation scheme of this passenger ship.

III. A. Analysis of information related to experimental subjects

III. A. 1) Statistics on research subjects

In this paper, we will analyze a real operating route of a shipping company in reality. The company is a ro-ro ship company, and the type of cargo loaded is mainly electric cars. On this route, the ship type and cabin are basically similar, and it is a liner operation, the date of shipment and the type and quantity of customer cargo sources are relatively stable, so a specific ship on the route is selected to do the experiment on the distribution of cargo operation. The starting point of the route Tianjin Port, midway port call Ningbo Port, the end of Guangzhou Port, a total of 3 ports, because the customer has requirements for the delivery of goods, midway to hang too many ports on the delivery of the risk of delay, so in reality such a long route from north to south is generally designed to hang a port in the middle of the route. The brand and quantity of vehicles to be loaded in each port are taken from the actual information of a certain voyage of the ship. Table 1 provides statistics on the information, quantity and size type of cargo to be loaded in each port. From the line as well as the vehicle length and width, the number of vehicles to be loaded, the line price, the line length, vehicle size and number, and the price of the line between the positive correlation between the line, that is, the longer the line, the larger the vehicle, the more vehicles, the higher the price of the line. For example, the same vehicle length and width, from Tianjin - Guangzhou loaded with 211 electric vehicles line price of 1401 yuan, while from Tianjin - Ningbo loaded with 191 electric vehicles line price is only 712 yuan. Also, therefore, in long-distance transportation, it is more important to consider the economic cost savings, and it is necessary to use the ant colony algorithm technique for the design of optimal transportation scheme.

Table 1: Information of goods to be loaded

Line	Vehicle number	Length (m)	Width (m)	Quantity to be installed	Line price
Tianjin - Guangzhou	A	4.74	1.73	211	1401
	B	4.45	1.71	112	1353
	C	5.01	1.92	315	1536
	D	4.67	1.74	1160	1405
Tianjin - Ningbo	A	4.74	1.73	193	712
	B	4.45	1.71	188	705
	C	5.01	1.92	165	708
	D	4.67	1.74	143	737
	E	4.61	1.75	301	719
Ningbo - Nansha	F	4.77	1.80	275	1205
	G	5.02	1.97	160	1284
	H	4.70	1.81	191	1207
	I	4.41	1.82	182	1202
	J	5.33	1.94	116	1305
	K	4.66	1.83	115	1206

III. A. 2) Information abstraction processing

Because of the definition in the mathematical model of this paper, the task of transportation is regarded as an OD pair number with loading demand (the OD pair contains the information of the starting port of the vehicle to be loaded, the destination port number information, the model number, the number of vehicles to be loaded, the length and width, as well as the price of the shipment), and in addition to the convenience of the program to read the data, some of the data are now simplified by the mathematical and theoretical abstraction. Table 2 is the experimental input data obtained after abstracting the information in Table 1. Tianjin port is the port number 1, Ningbo port is the port number 2, Nansha port is the port number 3; the model number according to the Tianjin departure 5 kinds of models sequentially numbered 1-5, Ningbo port departure 6 kinds of models numbered 6-11.

III. A. 3) Ship deck data analysis

After analyzing the data related to the EVs transported, the data is further integrated with the specific data of the passenger ships. Take a ship named AJ on this route as an example. This ship is an actual operating ro-ro ship, which has 8 decks, and Table 3 shows the parameters of each deck of the ship.The length of the 8 decks is between 90m-125m, and the width of the 8 decks is between 15m-20m, which is in line with the experimental requirements of this paper as it has the capability of transporting a large number of EVs and long-distance transportation of EVs.

Table 2: Experimental input data

OD pair numbers	Starting port number	Terminal port number	Vehicle model number	Quantity to be installed	Length (m)	Width (m)	Line price
1	1	3	1	211	4.74	1.73	1401
2	1	3	2	112	4.45	1.71	1353
3	1	3	4	315	5.01	1.92	1536
4	1	3	5	1160	4.67	1.74	1405
5	1	2	1	193	4.74	1.73	712
6	1	2	2	188	4.45	1.71	705
7	1	2	3	165	5.01	1.92	708
8	1	2	4	143	4.67	1.74	737
9	1	2	5	301	4.61	1.75	719
10	2	3	6	275	4.77	1.80	1205
11	2	3	7	160	5.02	1.97	1284
12	2	3	8	191	4.70	1.81	1207
13	2	3	9	182	4.41	1.82	1202
14	2	3	10	116	5.33	1.94	1305
15	2	3	11	115	4.66	1.83	1206

Table 3: Parameters of Layer A of AJ

DECK A (K)	Length (m)	Width (m)
1	90	15
2	95	15.5
3	100	16
4	105	17
5	110	18
6	115	20
7	120	20
8	125	20

III. B. Algorithm setup and effect analysis in the distribution scheme

III. B. 1) Effect of parameter combination (α,β) on the algorithm

In order to better find the optimal loading scheme for electric vehicles on passenger-roller ships, this paper uses the ant colony algorithm to solve the three sets of parameter combinations of information-inspired factor α and expectation-inspired factor β commonly used in loading optimization, which are $\alpha=1.2,\beta=2.0$, $\alpha=1.75,\beta=1.75$, and $\alpha=2.0,\beta=1.2$, respectively. The ACO algorithm proposed in this paper does 30 consecutive experiments with each of these 3 sets of parameter combinations and summarizes the results.

Figure 5 obtains the average convergence curves of the ACO algorithm under 3 groups of different parameter combinations. From the comparison graph of the iteration curves of different parameter combinations, it can be seen that the final convergence values of the 3 groups of parameters are different, but the convergence tends to be more or less the same. In the 1st to 5th iterations, the 3 groups of parameter combinations converge the fastest, and the objective function value stabilizes around the 21st generation. Among the three convergence curves, the combination of $\alpha=1.2,\beta=2.0$ has the smallest objective function value (the highest is not more than 280) and the fastest convergence speed (about 5 times that is, it reaches the basic stability), so the parameter combination selected in this paper is $\alpha=1.2,\beta=2.0$.

III. B. 2) Effect of ant population on the algorithm

The performance of the ant colony algorithm is affected by the configuration of the number of ants. If the number of ants is set too high, although it can improve the global exploration efficiency and stability of the algorithm, it will weaken the positive feedback effect and slow down the convergence rate of the algorithm at the same time; on the contrary, if the number of ants is too low, although it can speed up the convergence rate of the algorithm, its stochastic exploration ability will be significantly reduced, which may cause the algorithm to fall into the local optimum rather than the global optimum. In order to deeply explore the influence of the number of ants on the effect of the algorithm, the approach taken is to run the algorithm 30 times under seven common ant colony numbers (50, 55, 60, 65, 70, 75, 80) settings respectively, calculate the average value of the convergence data of each run, and then compare and analyze the convergence curves of these averages in detail.

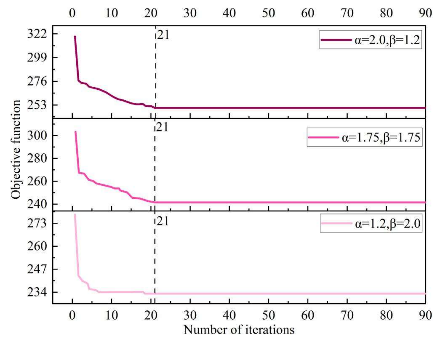

Figure 5: Iteration curve under three different parameter combinations

Fig. 6 shows the convergence curves of the ACO algorithm for different numbers of ant colonies. Under the seven common parameter settings of the number of ant colonies, although the final objective function values of the algorithm are different, the difference is not more than 10. Overall, it seems that the larger the number of ants, the smaller the objective function value, but after the number of ants is more than 65, the difference in the objective function value is even smaller. However, the larger the number of ants causes the algorithm's computing time to become longer, so in this paper, the number of ants is determined to be 65.

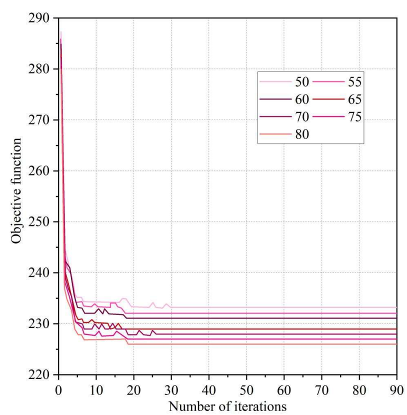

Figure 6: Convergence curves under different ant colony numbers

Based on the parameter experiments mentioned above, the specific parameter configurations of the improved particle swarm-ant colony joint optimization algorithm are as follows: the particle swarm size is 25, the constants a1, a2, b_1, b_2, f_1, f_2 are 1.5, the maximum value of inertia-weighting parameter w_1 is 0.85, the minimum value of inertia-weighting parameter w_2 is 0.45, the number of ant colonies kk is 65, the maximum number of iterations n max is 90, constant A is 1, pheromone strength Q is 550, constants σ_1, σ_2 are 2.0, information heuristic factor α is 1.2, and expectation heuristic factor β is 2.0.

III. B. 3) Algorithm convergence performance comparison

In order to verify the effectiveness of the ant colony algorithm in this paper for solving the large-scale electric vehicle transportation and loading scheme, the scenario of needing to transport electric vehicles exceeding the transportation volume of the passenger-roller ship is taken as a comparative experimental scenario, which is solved by the ant colony algorithm (AC), the particle swarm (PSO) algorithm, and the first-come, first-served (FCFS) algorithm, respectively, and compared with each other. Figure 7 represents the convergence curves of the simulation results comparing the three algorithms.

Comparing the convergence performance of the three algorithms, Ant Colony algorithm > Particle Swarm algorithm > First-Come-First-Served algorithm. The FCFS algorithm consistently maintains the objective function value above 310, which is the worst performance. The algorithm follows the first-come-first-served principle, i.e., the earliest arriving EVs are loaded first. Once the loading sequence of EVs on the RV is determined, this order is strictly maintained until the end of the line. This is the closest approach to manual loading, so the loading is not as effective as it could be. The particle swarm algorithm converges fast in 1-10 iterations, but it is easy to fall into a local optimum because the scenario is a large-scale dosing scenario with a high density of traffic. Ant colony algorithm converges the fastest and the maximum value of the objective function is less than 208, which has better distribution efficiency and results. According to the analysis of the comparison experiment, it is better to prove that the ant colony algorithm in this paper is better than other algorithms, both in the early convergence speed and the final objective function value. The ant colony algorithm can well synthesize and optimize the electric vehicle transportation scheme of the roll-on/roll-off ship, and achieve the maximum electric vehicle transportation capacity and the lowest economic cost at the same time.

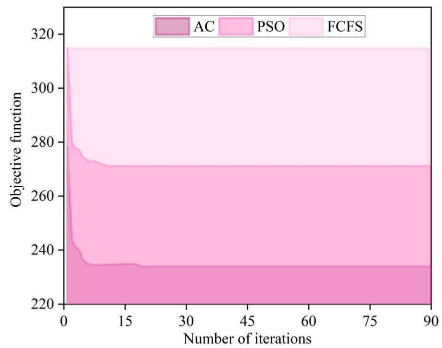

Figure 7: The convergence curves of the 3 comparison algorithms

III. C. Optimization of distribution scheme based on ant colony algorithm

After setting the parameters of the ACO algorithm and verifying the advantage of its convergence effect, the algorithm is used to solve the optimal loading scheme under 15 different transportation scenarios. f denotes the average value of the utilization rate of the loadable area on the cabin deck of the ro-ro ship for 15 times of each scenario run, and f' denotes the standard deviation of the results of the 15 experiments under each scenario.

Table 4 shows the statistics of the EV loading schemes for the 15 different scenarios of the roll-on/roll-off vessel. For the passenger roll-on/roll-off ship AJ with 8 decks, under different routes, different vehicle types and ratios, and different sizes of vehicles to be ferried, the utilization rate of the ship area of this passenger roll-on/roll-off ship reaches more than 95%, and the highest rate can reach 96.92%; at the same time, the standard deviation of the standard deviation is the maximum of 0.004, which is smaller than 0.005. It is proved that the used ant colony algorithm has a good stability, good solution performance, and can provide the electric vehicles for passenger roll-on/roll-off ships in the complex scenarios to provide the most fully utilized space and the least amount of ballast water for the passenger-roll-on ship with a loading scheme.

Table 4: Electric vehicle loading scheme for Ro-RO passenger ships

Serial number	Experimental scene	Experimental scale	f/%	f'
1	1-3-1	211	96.55	0.003
2	1-3-2	112	96.32	0.003
3	1-3-4	315	96.30	0.002
4	1-3-5	1160	96.55	0.001
5	1-2-1	193	95.27	0.002
6	1-2-2	188	95.56	0.004
7	1-2-3	165	95.93	0.003
8	1-2-4	143	95.42	0.002
9	1-2-5	301	96.31	0.001
10	2-3-6	275	96.65	0.004
11	2-3-7	160	96.36	0.004
12	2-3-8	191	96.92	0.003
13	2-3-9	182	96.47	0.002
14	2-3-10	116	96.52	0.004
15	2-3-11	115	96.21	0.001

IV. Conclusion

In this paper, the ant algorithm is used to calculate the optimal electric vehicle loading scheme for the passenger-roller ship, and the system improves the passenger-roller ship vehicle loading capacity and transportation stability. When the combination parameter α=1.2,β=2.0 is set, the objective function value of the ant algorithm is less than 280, and it starts to reach a stable state after converging about 5 times. When the number of ants is 65, the objective function value and running time are more balanced. In the comparison of the convergence performance of the three algorithms, the ant algorithm converges the fastest, and the objective function is optimal. 15 transportation scenarios of the average utilization rate of the passenger-roller ship deck loadable area can reach 96.92%, and the maximum standard deviation is only 0.004, the transportation optimization is effective. In the future, it can be accessed to the real-time monitoring of the vehicles to be loaded in each port to obtain the latest data situation, improve the calculation speed of the algorithm, and rapidly realize the optimization and updating of the loading scheme.

References

[1] Ančić, I., Vladimir, N., & Luttenberger, L. R. (2018). Energy efficiency of ro-ro passenger ships with integrated power systems. Ocean Engineering, 166, 350-357.

[2] Wang, X., Liu, Z., Zhao, Z., Wang, J., Loughney, S., & Wang, H. (2020). Passengers' likely behaviour based on demographic difference during an emergency evacuation in a Ro-Ro passenger ship. Safety science, 129, 104803.

[3] Manuel, T. A. S., & Soares, C. G. (2020). 2 Ro-Ro ships and dedicated short sea shipping. Short Sea Shipping in the Age of Sustainable Development and Information Technology.

[4] Fang, S., Liu, Z., Zhang, S., Wang, X., Wang, Y., & Ni, S. (2023). Evacuation simulation of an Ro-Ro passenger ship considering the effects of inclination and crew's guidance. Proceedings of the institution of mechanical engineers, part M: journal of engineering for the maritime environment, 237(1), 192-205.

[5] Hutchison, B. L. (2017, October). Capsize Egress and Survival with Particular Reference to RO-RO & Passenger Vessels. In SNAME Maritime Convention (p. D043S013R001). SNAME.

[6] Jovanović, I., Vladimir, N., Perčić, M., & Koričan, M. (2022). The feasibility of autonomous low-emission ro-ro passenger shipping in the Adriatic Sea. Ocean engineering, 247, 110712.

[7] Szymoński, M. (2024). Safety Management on Ro-Ro Passenger Ships. TransNav, International Journal on Marine Navigation and Safety od Sea Transportation, 18(2), 281-285.

[8] Szymoński, M. (2021). Stockholm agreement analysis for Ro-Ro passenger ships Navigating in the North European Waters and the Baltic Sea. TransNav: International Journal on Marine Navigation and Safety of Sea Transportation, 15(2), 427-435.

[9] Santos, T. A., & Guedes Soares, C. (2017). Methodology for ro-ro ship and fleet sizing with application to short sea shipping. Maritime Policy & Management, 44(7), 859-881.

[10] Ventura, M., Santos, T. A., & Soares, C. G. (2020). Ro-Ro ships and dedicated short sea shipping terminals. In Short sea shipping in the age of sustainable development and information technology (pp. 22-57). Routledge.

[11] Paulauskas, V., & Vytautas, D. (2020). Accuracy evaluation of Ro-Ro and Ro-Pax ships arrival to the ports. TransNav, International Journal on Marine Navigation and Safety od Sea Transportation, 14(2), 397-401.

[12] Agrawal, M., & Rajapatel, M. S. (2020). Global perspective on electric vehicle 2020. International Journal of Engineering Research & Technology, 9(1), 8-11.

[13] Mruzek, M., Gajdáč, I., Kučera, Ľ., & Gajdošík, T. (2017). The possibilities of increasing the electric vehicle range. Procedia engineering, 192, 621-625.

[14] Hemavathi, S., & Shinisha, A. (2022). A study on trends and developments in electric vehicle charging technologies. Journal of energy storage, 52, 105013.

[15] Figenbaum, E. (2017). Perspectives on Norway's supercharged electric vehicle policy. Environmental Innovation and Societal Transitions, 25, 14-34.

[16] Göksu, B. (2024). Stability of a Ro-Ro Ship: An Assessment of the Impact of Electric Vehicle Transportation. Journal of Marine and Engineering Technology, 4(1), 11-21.

[17] Şimşek, T., Sivri, F., Uğurlu, Ö., & Aydın, M. (2024). Forecasting Ro-Ro Freight Transportation Demand at Samsun Port: A Hybrid Method Approach. Turkish Journal of Maritime and Marine Sciences, 1-18.

[18] Furuichi, M., Kumazawa, K., & Shishido, T. (2017). ASEAN-wide connectivity by realizing RO/RO shipping network: Challenges and opportunities. Economic Integration and Regional Development, 147-161.

[19] Jiang, X., Ren, W., Xu, H., Zheng, S., & Wu, S. (2025). Mechanism-Based Fire Hazard Chain Risk Assessment for Roll-On/Roll-Off Passenger Vessels Transporting Electric Vehicles: A Fault Tree–Fuzzy Bayesian Network Approach. Journal of Marine Science & Engineering, 13(2).

[20] Zhao, Y., Peng, P., Zhou, J., & Wang, Y. (2025). Heuristic algorithm for integrated ship scheduling, routing and stowage problem in multi-vessel roll-on/roll-off shipping. Journal of Heuristics, 31(1), 15.

[21] Papanikolaou, A., Boulougouris, E., & Sklavenitis, A. (2014). The sinking of the Ro–Ro passenger ferry SS Heraklion. International Shipbuilding Progress, 61(1-2), 81-102.

[22] Skoupas, S., Zaraphonitis, G., & Papanikolaou, A. (2019). Parametric design and optimisation of high-speed Ro-Ro Passenger ships. Ocean Engineering, 189, 106346.

[23] Szymoński, M. (2023). Stability Control on Ro-Ro Passenger Ships as the Main Factor of Ship's Safety. Eur. J. Theor. Appl. Sci.,, 1(5), 1033-1041.

[24] Fancello, G., Serra, P., & Mancini, S. (2019). A network design optimization problem for ro-ro freight transport in the Tyrrhenian area. PROBLEMY TRANSPORTU, 14(4), 63-75.